



Published in final edited form as:

*Minim Invasive Ther Allied Technol.* 2016 June ; 25(3): 162–170. doi:10.3109/13645706.2015.1129970.

## Automatic bone removal for 3D TACE planning with C-arm CBCT: Evaluation of technical feasibility

Zhijun Wang<sup>a,b</sup>, Eberhard Hansis<sup>c</sup>, Rongxin Chen<sup>a</sup>, Rafael Duran<sup>a</sup>, Julius Chapiro<sup>a</sup>, Yun Robert Sheu<sup>a</sup>, Hicham Kobeiter<sup>d</sup>, Michael Grass<sup>c</sup>, Jean-François Geschwind<sup>e</sup>, and MingDe Lin<sup>e,f</sup>

<sup>a</sup>Russell H. Morgan Department of Radiology and Radiological Science, Division of Vascular and Interventional Radiology, The Johns Hopkins Hospital, Baltimore, MD, USA

<sup>b</sup>Interventional Radiology Department, Chinese PLA General Hospital, Beijing, China

<sup>c</sup>Philips Research, Hamburg, Germany

<sup>d</sup>Service d'Imagerie Médicale, Unité de Radiologie interventionnelle et thérapeutique Vasculaire et Oncologique, Université Paris-Est Créteil, Assistance Publique-Hôpitaux de Paris, Centre Hospitalo-Universitaire Henri Mondor, France

<sup>e</sup>Yale University School of Medicine, Department of Radiology and Biomedical Imaging, New Haven, CT, USA

<sup>f</sup>U/S Imaging and Interventions (UII), Philips Research North America, Cambridge, MA, USA

### Abstract

**Purpose**—To evaluate the technical feasibility of automatically removing the ribs and spine from C-arm cone-beam computed tomography (CBCT) images acquired during transcatheter arterial chemoembolization (TACE).

**Material and methods**—Fifty-eight patients ( $45.8 \pm 5.0$  years) with unresectable hepatocellular carcinoma (HCC) underwent transcatheter arterial chemoembolization and had intraprocedural CBCT imaging. Automatic bone removal was performed using model-based segmentation of the ventral cavity. Two interventional radiologists independently evaluated the performance of bone removal, remaining soft tissue retention, and general usability (where both the bone is appropriately removed while retaining soft tissue) for 3D TACE planning on a four-level (complete/excellent, adequate/good, incomplete/questionable, insufficient/bad) score. The proportion of inter-reader agreement was calculated.

**Results**—For ribs and spine removal, 98.3–100% and 100% of cases showed complete or adequate performance, respectively. In 96.6% of the cases, soft tissue was at least adequately retained. 91.3–93.1% of the cases demonstrated good or excellent general usability for TACE

---

**CONTACT** J.F. Geschwind, jeff.geschwind@yale.edu, Yale University School of Medicine, Department of Radiology and Biomedical Imaging 330 Cedar Street TE 2-230, New Haven, CT, USA.

#### Declaration of interest

The authors report no conflicts of interest. The authors alone are responsible for the content and writing of this paper.

planning. Satisfactory inter-reader agreement proportion was achieved in ribs (93.1%) and spine removal (89.7%), soft tissue retention (84.5%), and general usability for TACE planning (72.4%).

**Conclusion**—Intraprocedural automatic bone removal on CBCT images is technically feasible and offers good removal of ribs and spine while preserving soft tissue. Its clinical value needs further assessment.

### Keywords

Hepatocellular carcinoma; transcatheter arterial chemoembolization; cone-beam computed tomography; three-dimensional; automatic bone removal

## Introduction

Bony structures within the field of view in intra-procedurally acquired C-arm cone-beam CT (CBCT) imaging, in particular when 3D maximum intensity projection (MIP) reconstructions are used represent a challenge for interventional radiologists when performing vascular interventions in soft tissues close to the skeleton. As such, intra-procedural visualization of small vascular structures close to the spinal column, pelvis or the rib cage may impede correct catheter placement. One such procedure is transcatheter arterial chemoembolization (TACE) for the treatment of unresectable hepatocellular carcinoma (HCC) tumors. Generally, TACE can be performed in either a selective or non-selective (lobar or segmental catheterization) intra-arterial catheterization manner. While the non-selective manner is workflow-efficient, the selective method, and especially superselective (catheterization up to the sole vessel feeding the tumor) TACE, has the benefit of avoiding damage to the nontumoral liver parenchyma and, in comparison to nonselective TACE, has been shown to have better short-term effects and increased long-term survival (1–3). The proper identification and catheterization of tumor-feeding arteries is very important for successful superselective embolization, which was previously achieved using two-dimensional (2D) imaging only, specifically fluoroscopy and digital subtraction angiography (DSA). However, some tumors and their feeding arteries can be difficult to detect, identify and catheterize using 2D projection imaging (4). Possible reasons are overlapping blood vessels, insufficient tumor vascularity, small tumors, low dynamic range, and reduced hypervascularity after several TACE procedures. This can lead to misidentification of the feeding artery and incorrect or suboptimal catheterization (3,5). A recent solution is the use of intraprocedural CBCT imaging. Compared with 2D standard angiography and guidance, CBCT has shown several advantages: It provides more information on tumor detection and localization, intraprocedural 3D guidance for catheter/micro-catheter positioning, and intraprocedural assessment of embolization success (5–10). As such, the use of CBCT during TACE has been shown to improve survival (11). It has been suggested that the 3D CBCT guidance planning workflow during TACE should include a dual phase CBCT scan, tumor segmentation, bone (ribs and spine) removal and feeding artery identification (12,13). TACE with 3D CBCT guidance technology can help the interventional radiologist to find tumor feeding arteries and thus catheterize them more easily (13–15). However, surrounding bone (ribs and spine) can obscure the vessels, making visualization difficult. Therefore, manual bone masking is often necessary to achieve an unobstructed visualization of the

vessel (14). However, this manual process adds another layer of user interaction and makes the workflow of TACE planning less time-efficient (16). To address this limitation, we developed a fully automatic bone removal software as described in previous work (17). The purpose of our study is to assess the technical feasibility of automatic bone removal for 3D TACE planning.

## Material and methods

### Patient selection

This was a two-institution retrospective analysis of prospectively collected data. The Health Insurance Portability and Accountability Act (HIPPA) compliant and Institutional Review Board (IRB) approved. All patients were provided with informed consent before inclusion into the study. The diagnosis of HCC was confirmed by biopsy or by typical radiologic findings in addition to an increased serum alpha-fetoprotein level [ $>200$  ng/ml]. All patients were treated for unresectable HCC after discussion at the institution's multidisciplinary liver conference. Eligibility criteria for TACE were as follows: uni- or multifocal HCC, Child-Pugh classification A or B, Eastern Cooperative Oncology Group performance status 0 or 1, absence or traces of ascites; albumin  $>2.5$  g/dl; alanine aminotransferase and aspartate aminotransferase  $<5$  times the upper normal limit; total serum bilirubin  $<3.0$  mg/dl; serum creatinine  $<2.0$  mg/dl; platelet count  $>50,000/\text{mm}^3$ ; international normalized ratio (INR) 1.5; no contraindication to iodinated contrast. Exclusion criteria were tumor burden  $>70\%$ , presence of extrahepatic disease, or complete tumor occlusion of portal vein, or no intraprocedural CBCT imaging. Patients receiving at least one dual phase intra-procedural CBCT scan were included in this study.

From August 2011 to September 2012, 38 patients from the USA and 20 patients from France underwent segmental or subsegmental TACE. Patient characteristics are described in Table 1. In this study, all 58 patients for automatic bone removal assessment met the same inclusion and exclusion criteria for TACE. CBCT acquisitions were performed in 13 cases at the level of the celiac artery, 11 at the level of the common hepatic artery, 11 at the level of the proper hepatic artery, 12 at the level of the right hepatic artery, and 11 at the level of the left artery.

### Intraprocedural dual phase CBCT technique

All patients underwent C-arm dual-phase CBCT imaging during hepatic arteriography before TACE therapy. CBCT was performed using a commercially available angiographic system (Allura Xper FD20, Philips Healthcare, Best, The Netherlands) with the XperCT option, enabling CBCT acquisition and volumetric image reconstruction (Feldkamp backprojection). For each CBCT scan, the area of interest was positioned in the system center and in approximately 5s, 312 projection images (30frames/s) were acquired with the motorized C-arm covering a  $200^\circ$  clockwise arc at a  $40^\circ/\text{s}$  rotation speed under a fixed 120-kVp, 50-mA, 3-ms setting. As the images were being acquired, the projections were transferred to the reconstruction computer. The 2D projection images were reconstructed using Feldkamp backprojection into 3D volumetric images (17–19) with an isotropic resolution of 0.65 mm for a  $250 \times 250 \times 194 \text{ mm}^3$  field of view (FOV) (matrix size  $384 \times$

384 × 298). The dual-phase CBCT prototype uses a modified XperCT protocol for the acquisition of two sequential, back-to-back CBCT scans, so both arterial and delayed arterial phases are captured using only one contrast injection (20). In this study, the two scans were triggered at three and 28 seconds after a selective single injection of undiluted contrast medium. A 5F SIM-1 catheter (Angiodynamics, Latham, NY, USA) was used if the injection location was from the celiac artery or the common hepatic artery or a 3F Renegade High-Flo microcatheter (Boston Scientific, Natick, MA, USA) was used if the injection location was from the proper, right, or left hepatic artery. The contrast injection protocol was as follows: 20 ml at 2 ml/s for the celiac artery and the common hepatic artery; 15 ml at 1.5 ml/s for the right or left hepatic artery (Oxilan, Guerbet LLC, Bloomington, IN, USA). Bone removal was evaluated on the arterial phase volume only, since this is used for feeding arteries visualization and detection.

### Automatic bone removal

Automatic bone removal was performed using prototype software which uses a model-based segmentation of the ventral cavity (17). Briefly, a surface model of the ventral cavity which delineates the boundary between the interior organs and the rib cage and spine is used (21). In the anterior abdominal area, the model is suitably extended downward from the rib cage, including all interior organs but excluding the spine. The model is automatically adapted to a specific target image, using a shape-constrained deformable model with learned boundary features (22,23). Boundary features are selected from a set of candidate features and trained to optimize robustness and accuracy of the model adaptation. This training was done by providing ground truth through manual segmentation of 30 cases by a radiologist with eight years of experience who did not participate in the TACE procedure, as published previously (17). For this study, another 58 cases were obtained from the same institutions. The manual portion of the study was for creating a trained segmentation model from which the automatic segmentation could then be applied to the study patients. Initialization of the model is performed by automatic detection of the spinal column and corresponding positioning and bending of the model. This is followed by the deformable model adaptation. In previous work, it was shown that the automatic segmentation of the ventral cavity can achieve an average mesh-to-mesh distance of  $2.7 \pm 5.4$  mm when compared to manual segmentation (17). After adaptation, the model exterior is masked to achieve bone removal. In other words, only the interior of the ventral cavity is retained for visualization, masking the bones outside of it. The software works automatically (<1 sec) and eliminates the need for manual interaction.

### Assessment

For each case, images before and after automatic bone removal were visualized side-by-side. Image properties were assessed by two interventional radiologists (Reader1: five years of experience and Reader2: nine years of experience) that did not participate in the TACE procedure. Images after bone removal (ribs and spine) were assessed on a four-level score, using the questionnaire shown in Table 2. The different grades of general usability for TACE were classified from “excellent” to “bad”, which is described in detail below. For bone removal, “complete” represented no remaining bones (Figure 1A–D; Figure 2A1–A2); “adequate” indicated a small amount of remainders that obstructed non-relevant vasculature

in a limited view range (Figure 2B1–B2); “incomplete” indicated a medium amount of remainders that obstructed tumor feeding arteries in a limited view range, and “insufficient” indicated substantial remainders that obstructed a substantial portion of the tumor-feeding vasculature. We used the parameter of soft tissue retention to assess the effect of bone removal on unintentional removal of soft tissue. For soft tissue retention (i.e. healthy liver tissue, vessels and tumor), “complete” indicated no soft tissue was unintentionally removed; “adequate” indicated no tumor or vessel was removed and only minimal removal of liver tissue; “incomplete” indicated no tumor or vessel was removed and a moderate removal of liver tissue or minimal removal of liver tissue which is adjacent to tumor (Figure 2C1–C2), and “insufficient” indicated removal of vessels or tumor, irrespective of liver tissue. For general usability in TACE planning, it indicated the benefit of the CBCT images after bone removal while retaining soft tissue information for 3D TACE planning. A four-level scoring of general usability after bone removal for 3D TACE planning is shown in Table 3 and examples of the different grades from “excellent” to “bad” are described in detail in Figure 2. If general usability for TACE planning after bone removal was questionable or bad, the readers were further asked to assess general image quality to find the potential factors that affect image quality apart from automatic bone removal.

## Statistics

To better understand the results, a conversion was performed to allow binary classification into “satisfactory” and “unsatisfactory”, “complete” and “adequate” or “excellent” and “good” were combined into “satisfactory”; “incomplete” and “insufficient” or “questionable” and “bad” were combined into “unsatisfactory”. The proportion of “satisfactory” and “unsatisfactory” responses was calculated for each reader and parameter. The proportion of inter-reader agreement in a four-level score and a combined two-level score were also calculated for each parameter. All data analysis was performed with STATA Statistical Software, Release 11.0 (College Station, TX, USA).

## Results

### Results of bone removal for 3D TACE planning

For ribs and spine removal, 98.3–100% of cases and 100% of cases showed complete or adequate removal, respectively. 96.6% of cases showed at least adequate retention of the soft tissue. 91.3–93.1% of cases obtained at least good performance in general usability for TACE planning after bone removal (Table 4). The remaining 6.9–8.7% of cases with questionable or bad scores included those with unsatisfactory ribs removal (one case, Reader2), soft tissue removal (two cases, Reader 1&2), sub-optimal image quality due to inadequate execution of acquisition (e.g. delay in image acquisition after contrast injection) and/or contrast injection protocols (2 cases, Reader1&2). One case was found (by Reader 1) for which a small part of the liver was not included in the CBCT; however, this did not affect the image usability for TACE planning. The limitation of a small field of view in CBCT imaging could be solved using a liver-centered CBCT acquisition to be able to image the entire liver (24). Example results from bone removal are shown in Figure 1.

When using a four-level score, satisfactory inter-reader agreement was achieved in ribs and spine removal, soft tissue retention, and general usability after bone removal for TACE planning. 93.1% inter-reader agreement was obtained in ribs removal, 89.7% inter-reader agreement was obtained in spine removal, 84.5% inter-reader agreement was obtained in soft tissue retention and 72.4% inter-reader agreement was obtained in general usability after bone removal for TACE planning.

Using a combined two-level score, a more satisfactory inter-reader agreement was achieved in the above four parameters. 98.3% inter-reader agreement was obtained in rib removal, 100% inter-reader agreement was obtained in spine removal, 100% inter-reader agreement was obtained in soft tissue retention and 100% inter-reader agreement was obtained in general usability after bone removal for TACE planning.

## Discussion

The main findings of our study are that there is a satisfactory removal of ribs and spine (>98%), while preserving soft tissue (96.6%) when using the automatic bone removal software. A high degree of general usability was achieved (>91.3%) for 3D TACE guidance. In addition, a satisfactory inter-reader agreement proportion for all parameters using a four-level score (>70%) was found.

Superselective TACE has been shown to be beneficial for patients with unresectable HCC (1–3,5). TACE with CBCT assistance has demonstrated several distinct advantages over 2D imaging including the identification and visualization of the tumor-feeding artery, which can be especially challenging for small tumors and for reduced hypervascularity after several TACE sessions (8,15,16,23,25–26). 3D guidance technology that uses CBCT is capable of automatic feeding artery identification and 3D guidance (14–16). 3D CBCT guidance workflow during TACE was suggested to include dual phase CBCT imaging, tumor segmentation, manual bone removal and feeding artery identification (12,13). The whole process usually takes several minutes and requires an involved manual interaction. Thus, it has been challenging to use 3D image guidance routinely, especially when compared to real-time 2D imaging, even with several methods that can accelerate the workflow through the automatic identification of tumor-feeding arteries (5,14–16,27). Furthermore, bone (ribs and spine) that obstructs the visualization of the tumor and its feeding vessels is another factor that affects routine use of intraprocedural CBCT guidance. Removing bone can improve the visibility of vessels and benefit 3D guidance, especially when the tumor is small, located peripherally, and needs superselective TACE. Bone masking is currently done manually. However, this manual process adds another layer of user interaction and makes the overall process of identifying the feeding artery and TACE planning workflow inefficient. A number of automatic bone segmentation methods have been described in the past. However, many of them use gray-value-based thresholding which could also remove contrast-enhanced vessels, reducing the general usability for TACE planning (28,29). Other methods rely on watershed segmentation with manual corrections (30,31). For CT angiography, special acquisition protocols are used, such as performing both a contrast and a non-contrast scan with subsequent subtraction or using a dual-energy acquisition for bone separation (32–35). Such

methods cannot be applied with the present CBCT imaging systems and acquisition protocols. Furthermore, this increases the amount of radiation exposure of the patient.

There exist model-based methods for segmentation of certain bone structures, such as the rib cage and spine with great accuracy (36–37). While such methods could in principle be used for bone removal, what is required is not a complete and accurate delineation of the bones, but just their removal while retaining the soft tissue anatomy of interest. Furthermore, these methods have a computation time penalty, on the order of minutes, and thus do not contribute much to workflow efficiency. The presented method is the leading solution because it is conceptually simple and thus is computationally efficient, and robust in the terms of anatomical variation, especially in the presence of contrast agent filled vessels. More importantly, the underlying technology of the presented method is easily translatable from transcatheter vascular interventions to other regions of the body such as the pelvis, skull base or the spinal column.

The technical performance of the bone removal method used in our study was evaluated in a previous study on 30 patient cases by quantitatively comparing its accuracy to manual segmentation (17). The main finding was that the mean mesh-to-mesh distance between manual and automatic bone segmentation was 2.7 mm, with best performance in the spine area (1.1 mm) and worst in the anterior portion of the CBCT volumes (4.4 mm). Our study focused on the technical feasibility of applying such software and it was found to have satisfactory bone removal performance while retaining soft tissue. A satisfactory inter-reader agreement proportion was obtained for all parameters when using both a four-level score and a combined two-level score. When using a combined two-level score, more satisfactory inter-reader agreement was achieved than when using a four-level score. This can be attributed to the following two factors: First, the categories were qualitative, not quantitative. Second, the different scores between Reader1 and Reader2 for the same image usually occurred between “excellent” and “good”, or “questionable” and “bad”, not between “good” and “questionable”. For example, in some images, Reader1 gave an “excellent” score whereas Reader2 gave a “good” score. Satisfactory automatic bone removal performance and inter-user agreement shows its feasibility and repeatability in different readers. The study results demonstrate that automatic software is technically feasible, and it could optimize the workflow of 3D CBCT guidance for TACE.

Several factors affect general usability such as the dual phase CBCT protocol and the performance of automatic bone removal. In this study, there was a high degree (91.3–93.1%) of general usability for TACE planning with both readers. However, Reader 1 reported 6.9% and Reader 2 reported 8.7% of the cases in our study could not be visualized well and were judged as unusable for 3D TACE planning. Sub-optimal image acquisition and/or contrast injection protocols were the major source of poor image quality, which is independent of automatic bone removal.

There were some limitations in this study. First, the parameters were subjective (qualitative) and not quantitative, but this is an inherent limitation of reading studies. Second, the processing was done offline and retrospectively. Utilization of the method during a

prospective study would be beneficial. However, the scope of our study as the first step in introducing this method was to show feasibility.

## Conclusion

Intraoperative automatic bone removal on CBCT images is technically feasible, workflow efficient, and offers good removal of ribs and spine while preserving soft tissue in the majority of patients. Its clinical value needs further assessment in a prospective study to evaluate how this technique might alter the management/change in catheter position.

## Acknowledgments

We would like to acknowledge Carol B. Thompson, Biostatistics Center, The Johns Hopkins Bloomberg School of Public Health for her help with the statistical analysis as supported by the National Center for Research Resources and the National Center for Advancing Translational Sciences (NCATS) of the National Institutes of Health through Grant Number 101872

Support for this work was provided by NIH/NCI R01 CA160771, P30 CA006973, Philips Research North America, Cambridge, MA, USA, the Rolf W. Guenther Foundation for Radiological Science, and the Beijing Nova Program (Z121107002512127)

## References

1. Yamakado K, Miyayama S, Hirota S, Mizunuma K, Nakamura K, Inaba Y, et al. Hepatic arterial embolization for unresectable hepatocellular carcinomas: do technical factors affect prognosis? *Jpn J Radiol.* 2012; 30:560–566. [PubMed: 22644412]
2. Miyayama S, Mitsui T, Zen Y, Sudo Y, Yamashiro M, Okuda M, et al. Histopathological findings after ultra-selective transcatheter arterial chemoembolization for hepatocellular carcinoma. *Hepatol Res.* 2009; 39:374–381. [PubMed: 19054146]
3. Iwamoto S, Yamaguchi T, Hongo O, Iwamoto H, Sanefuji H. Excellent outcomes with angiographic subsegmentectomy in the treatment of typical hepatocellular carcinoma: a retrospective study of local recurrence and long-term survival rates in 120 patients with hepatocellular carcinoma. *Cancer.* 2010; 116:393–399. [PubMed: 19908259]
4. Scherthaner R, Lin M, Duran R, Chapiro J, Wang Z, Geschwind JF. Delayed-phase Cone-Beam CT improves detectability of intrahepatic cholangiocarcinoma during conventional transarterial chemoembolization. *Cardiovasc Intervent Radio.* 2015; 38:929–936.
5. Deschamps F, Solomon SB, Thornton RH, Rao P, Hakime A, Kuo V, et al. Computed analysis of three-dimensional Cone-Beam computed tomography angiography for determination of tumor-feeding vessels during chemoembolization of liver tumor: A pilot study. *Cardiovasc Intervent Radiol.* 2010; 33:1235–1242. [PubMed: 20390271]
6. Miyayama S, Yamashiro M, Hattori Y, Orito N, Matsui K, Tsuji K, et al. Efficacy of cone-beam computed tomography during transcatheter arterial chemoembolization for hepatocellular carcinoma. *Jpn J Radiol.* 2011; 29:371–377. [PubMed: 21786092]
7. Tognolini A, Louie J, Hwang G, Hofmann L, Sze D, Kothary N. C-arm computed tomography for hepatic interventions: a practical guide. *J Vasc Interv Radiol.* 2010; 21:1817–1823. [PubMed: 20970354]
8. Lin M, Loffroy R, Noordhoek N, Taguchi K, Radaelli A, Blijd J, et al. Evaluating tumors in transcatheter arterial chemoembolization (TACE) using dual-phase cone-beam CT. *Minim Invasive Ther Allied Technol.* 2011; 20:276–281. [PubMed: 21082901]
9. Loffroy R, Lin M, Yenokyan G, Rao PP, Bhagat N, Noordhoek N, et al. Intraoperative C-arm dual-phase cone-beam CT: can it be used to predict short-term response to TACE with drug-eluting beads in patients with hepatocellular carcinoma? *Radiology.* 2013; 266:636–648. [PubMed: 23143027]

10. Wang Z, Lin M, Lesage D, Chen R, Chapiro J, Gu T, et al. Three-dimensional evaluation of lipiodol retention in HCC after chemoembolization: A quantitative comparison between CBCT and MDCT. *Acad Radiol.* 2014; 21:393–399. [PubMed: 24507426]
11. Iwazawa J, Ohue S, Hashimoto N, Muramoto O, Mitani T. Survival after c-arm CT-assisted chemoembolization of unresectable hepatocellular carcinoma. *Eur J Radiol.* 2012; 81:3985–3992. [PubMed: 22959287]
12. Tacher V, Radaelli A, Lin M, Geschwind JF. How I do it: Cone beam computer tomography during transarterial chemoembolization for liver cancer. *Radiology.* 2015; 274:320–334. [PubMed: 25625741]
13. Tacher V, Lin M, Bhagat N, Radaelli A, Noordhoek N, Carelsen B, et al. Dual-phase cone-beam computed tomography to see, reach, and treat hepatocellular carcinoma during drug-eluting beads transarterial chemo-embolization. *Journal of visualized experiments: JoVE.* 2013; 82:50795. [PubMed: 24326874]
14. Miyayama S, Yamashiro M, Hashimoto M, Hashimoto N, Ikuno M, Okumura K, et al. Identification of small hepatocellular carcinoma and tumor-feeding branches with cone-beam CT guidance technology during transcatheter arterial chemoembolization. *J Vasc Interv Radiol.* 2013; 24:501–508. [PubMed: 23452552]
15. Wang X, Shah RP, Maybody M, Brown KT, Getrajdman GI, Stevenson C, et al. Cystic artery localization with a three-dimensional angiography vessel tracking system compared with conventional two-dimensional angiography. *J Vasc Interv Radiol.* 2011; 22:1414–1419. [PubMed: 21546264]
16. Iwazawa J, Ohue S, Hashimoto N, Muramoto O, Mitani T. Clinical utility and limitations of tumor-feeder detection software for liver cancer embolization. *Eur J Radiol.* 2013; 82:1665–1671. [PubMed: 23743053]
17. Hansis ERA, Noordhoek N, Grass M. Automatic bone removal for 3D liver TACE planning with C-arm CT. *Proc IEEE ISBI.* 2013:1408–1411.
18. Feldkamp LADLC, Kress JW. Practical cone-beam algorithms. *J Opt Soc Am.* 1984; A6:612–619.
19. Grass M, Koppe R, Klotz E, Proksa R, Kuhn MH, Aerts H, et al. Three-dimensional reconstruction of high contrast objects using C-arm image intensifier projection data. *Comput Med Imaging Graph.* 1999; 23:311–321. [PubMed: 10634143]
20. Lorenz C, Schäer D, Eshuis P, Carroll J, Grass M. Automated volume of interest delineation and rendering of cone beam CT images in interventional cardiology. *Proc SPIE.* 2012:8316.
21. Ecabert O, Peters J, Schramm H, Lorenz C, von Berg J, Walker MJ, et al. Automatic model-based segmentation of the heart in CT images. *IEEE Trans Med Imaging.* 2008; 27:1189–1201. [PubMed: 18753041]
22. Peters J, Ecabert O, Meyer C, Kneser R, Weese J. Optimizing boundary detection via Simulated Search with applications to multi-modal heart segmentation. *Med Image Anal.* 2010; 14:70–84. [PubMed: 19931481]
23. Miyayama S, Yamashiro M, Okuda M, Yoshie Y, Sugimori N, Igarashi S, et al. Usefulness of cone-beam computed tomography during ultraselective transcatheter arterial chemoembolization for small hepatocellular carcinomas that cannot be demonstrated on angiography. *Cardiovasc Intervent Radiol.* 2009; 32:255–264. [PubMed: 19067043]
24. Scherthaner R, Chapiro J, Sahu S, Withagen P, Duran R, Sohn J, et al. Feasibility of a modified cone-beam CT rotation trajectory to improve liver periphery visualization during transarterial chemoembolization. *Radiology.* 2015; 277:833–841. [PubMed: 26000642]
25. Abdelmaksoud MH, Louie JD, Hwang GL, Sze DY, Hofmann LV, Kothary N. Transarterial chemoembolization for hepatocellular carcinomas in watershed segments: utility of C-arm computed tomography for treatment planning. *J Vasc Interv Radiol.* 2012; 23:281–283. [PubMed: 22264556]
26. Kakeda S, Korogi Y, Ohnari N, Moriya J, Oda N, Nishino K, et al. Usefulness of cone-beam volume CT with flat panel detectors in conjunction with catheter angiography for transcatheter arterial embolization. *J Vasc Interv Radiol.* 2007; 18:1508–1516. [PubMed: 18057285]

27. Meyer BC, Witschel M, Frericks BB, Voges M, Hopfenmüller W, Wolf KJ, et al. The value of combined soft-tissue and vessel visualisation before transarterial chemoembolisation of the liver using C-arm computed tomography. *Eur Radiol.* 2009; 19:2302–2309. [PubMed: 19424701]
28. Kang Y, Engelke K, Kalender WA. A new accurate and precise 3-D segmentation method for skeletal structures in volumetric CT data. *IEEE transactions on medical imaging.* 2003; 22:586–598. [PubMed: 12846428]
29. Wang LI, Greenspan M, Ellis R. Validation of bone segmentation and improved 3-D registration using contour coherency in CT data. *IEEE transactions on medical imaging.* 2006; 25:324–334. [PubMed: 16524088]
30. Hahn HKWMT, Drexler J, et al. HWT-hybrid watershed transform: optimal combination of hierarchical interactive and automated image segmentation. In *Proc SPIE Med Imag.* 2007:65120Z–Z.
31. Heath DG, Hahn HK, Johnson PT, Fishman EK. Automated multidetector row CT dataset segmentation with an interactive watershed transform (IWT) algorithm: Part 1. Understanding the IWT technique. *Journal of digital imaging.* 2008; 21:408–412. [PubMed: 18060525]
32. Johnson PT, Hahn HK, Heath DG, Fishman EK. Automated multidetector row CT dataset segmentation with an interactive watershed transform (IWT) algorithm: Part 2. Body CT angiographic and orthopedic applications. *Journal of digital imaging.* 2008; 21:413–421. [PubMed: 18066625]
33. Van Straten M, Venema HW, Streekstra GJ, Majoie CB, den Heeten GJ, Grimbergen CA. Removal of bone in CT angiography of the cervical arteries by piecewise matched mask bone elimination. *Medical physics.* 2004; 31:2924–2933. [PubMed: 15543801]
34. Tomandl BF, Hammen T, Klotz E, Ditt H, Stemper B, Lell M. Bone-subtraction CT angiography for the evaluation of intracranial aneurysms. *Am J Neuroradiol.* 2006; 27:55–59. [PubMed: 16418356]
35. Deng K, Liu C, Ma R, Sun C, Wang XM, et al. Clinical evaluation of dual-energy bone removal in CT angiography of the head and neck: comparison with conventional bone-subtraction CT angiography. *Clin Radiol.* 2009; 64:534–541. [PubMed: 19348851]
36. Klinder T, Lorenz C, von Berg J, Dries SP, Bulow T, Ostermann J. Automated model-based rib cage segmentation and labeling in CT images. *Medical image computing and computer-assisted intervention: MICCAI International Conference on Medical Image Computing and Computer-Assisted Intervention.* 2007; 10:195–202.
37. Klinder T, Ostermann J, Ehm M, Franz A, Kneser R, Lorenz C. Automated model-based vertebra detection, identification, and segmentation in CT images. *Medical image analysis.* 2009; 13:471–482. [PubMed: 19285910]

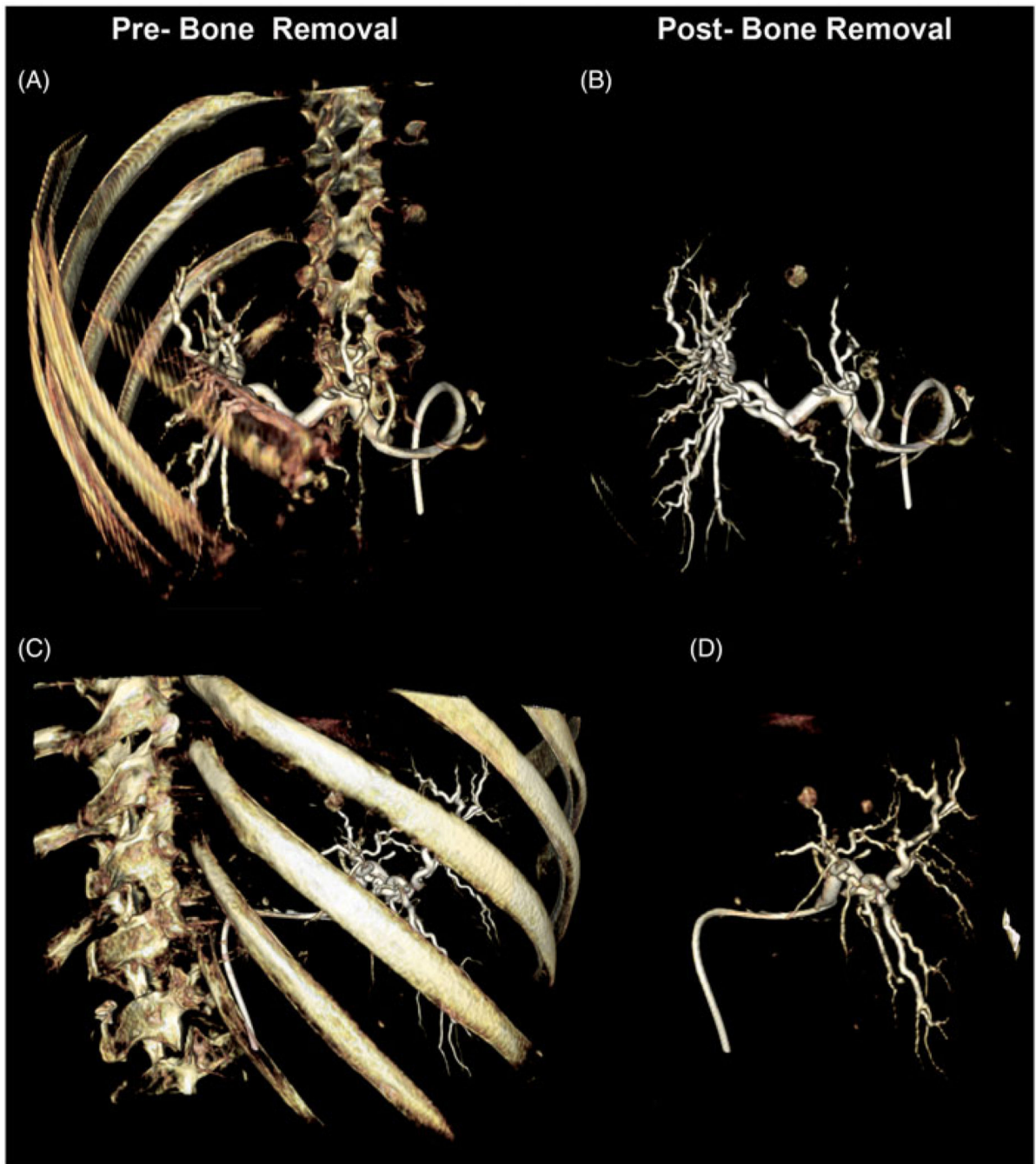


**Figure 1.**  
Example case before (A and C) and after (B and D) complete bone removal shown as a volume rendering at two orientations (top and bottom rows).

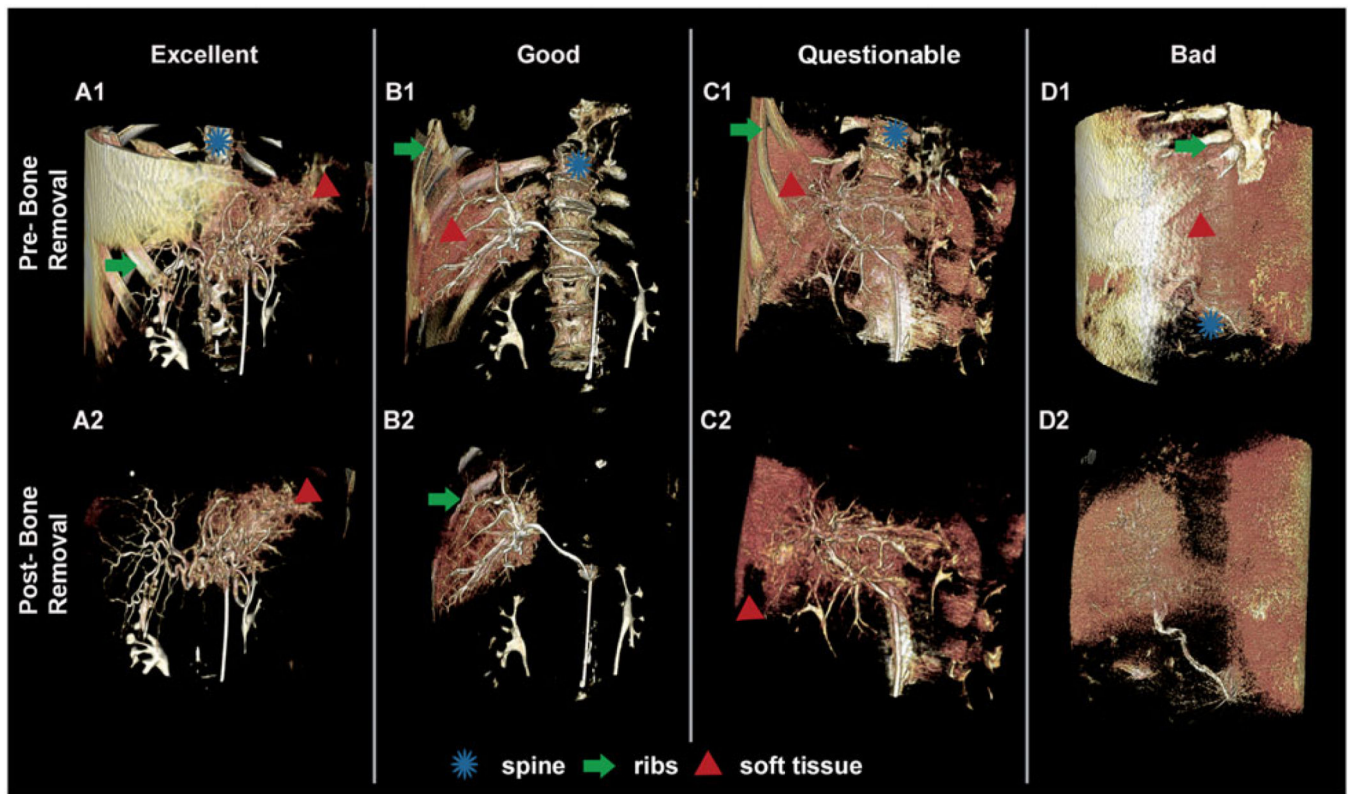


**Figure 2.**

Examples of before and after bone removal with different grades from “Excellent” to “Bad”. The pointers refer to notable image visualization features of the spine (\*), ribs (arrow), and soft tissue (triangle).

**Table 1**

Baseline patient characteristics.

Parameter	Value
No. of patients	58
Age(y) *	45.8 ± 5.0
Sex	
Male	35
Female	23
Etiology	
Hepatitis B virus	19
Hepatitis C virus	28
Other	11
Diagnosis	
Clinical	13
Pathological	45
Disease pattern	
Unifocal	14
Bifocal	14
Multifocal	30
Child-Pugh class	
A	32
B	26
Barcelona Clinic Liver Cancer stage	
A	17
B	41
ECOG	
0	25
1	33
Position of catheter	
Celiac artery	13
Common hepatic artery	11
Proper hepatic artery	11
Right/left hepatic artery	12/11

\*Data are expressed as means ± standard deviations

**Table 2**

Questionnaire for readers on scoring the image quality on a four-level scale (mark respective score).

	Complete	Adequate	Incomplete	Insufficient
How much of the ribs was removed				
How much of the spine was removed				
Which amount of relevant soft tissue is retained after bone removal				
	Excellent	Good	Questionable	Bad
General usability after bone removal for TACE planning				

Author Manuscript

Author Manuscript

Author Manuscript

Author Manuscript

**Table 3**

A four-level scoring of general usability after bone removal for 3D TACE planning.

Bone removal		Relevant soft tissue retained			General usability			
Complete	Adequate	Incomplete	Insufficient	Complete	Adequate	Incomplete	Insufficient	General usability
								Excellent
								Good
								Questionable
								Bad

**Table 4**

Automatic bone removal evaluation results.

Parameters	Reader 1					Reader 2				
	Complete (n)	Adequate (n)	Incomplete (n)	Insufficient (n)	Bad (n)	Complete (n)	Adequate (n)	Incomplete (n)	Insufficient (n)	Bad (n)
Ribs removed	50	8	0	0	0	51	6	1	0	0
Spine removed	53	5	0	0	0	55	3	0	0	0
Relevant soft tissue retained	51	5	0	2	2	54	2	2	0	0
	Excellent (n)	Good (n)	Questionable (n)	Bad (n)	Bad (n)	Excellent (n)	Good (n)	Questionable (n)	Bad (n)	Bad (n)
General usability for TACE planning	37	17	2	2	2	40	13	4	1	1